Journal of Zhejiang University-SCIENCE B (Biomedicine & Biotechnology)
ISSN 1673-1581 (Print); ISSN 1862-1783 (Online)
www.jzus.zju.edu.cn; www.springerlink.com
E-mail: jzus@zju.edu.cn

# Hyaluronic acid derivative-modified nano-structured lipid carrier for cancer targeting and therapy*#

Xiao LIU†1, Hai LIU[2], Su-lan WANG[1], Jing-wen LIU[3]

[1]*Department of Pharmacy, Sir Run Run Shaw Hospital, School of Medicine, Zhejiang University, Hangzhou 310016, China*

[2]*Department of Radiotherapy, Sir Run Run Shaw Hospital, School of Medicine, Zhejiang University, Hangzhou 310016, China*

[3]*Department of Pharmacological and Pharmaceutical Sciences, College of Pharmacy, University of Houston, Houston TX 77030, USA*

†E-mail: 3415120@zju.edu.cn

Received Dec. 8, 2019; Revision accepted Mar. 20, 2020; Crosschecked June 5, 2020

**Abstract:** To reduce the problems of poor solubility, high in vivo dosage requirement, and weak targeting ability of paclitaxel (PTX), a hyaluronic acid-octadecylamine (HA-ODA)-modified nano-structured lipid carrier (HA-NLC) was constructed. HA-ODA conjugates were synthesized by an amide reaction between HA and ODA. The hydrophobic chain of HA-ODA can be embedded in the lipid core of the NLC to obtain HA-NLC. The HA-NLC displayed strong internalization in cluster determinant 44 (CD44) highly expressed MCF-7 cells, and endocytosis mediated by the CD44 receptor was involved. The HA-NLC had an encapsulation efficiency of PTX of 72.0%. The cytotoxicity of the PTX-loaded nanoparticle HA-NLC/PTX in MCF-7 cells was much stronger than that of the commercial preparation Taxol®. In vivo, the HA-NLC exhibited strong tumor targeting ability. The distribution of the NLCs to the liver and spleen was reduced after HA modification, while more nanoparticles were aggregated to the tumor site. Our results suggest that HA-NLC has excellent properties as a nano drug carrier and potential for in vivo targeting.

**Key words:** Paclitaxel (PTX); Hyaluronic acid-octadecylamine (HA-ODA); Nano-structured lipid carrier (NLC); Tumor targeting; In vivo distribution

https://doi.org/10.1631/jzus.B1900624 **CLC number:** R94; TB383

## 1 Introduction

Paclitaxel (PTX) is a first-line drug for clinical treatment of ovarian and breast cancers (Bourgeois-Daigneault et al., 2016), but its application is limited because of poor solubility and the requirement for a large dosage in vivo. Current commercial formulations include Paclitaxel®, Taxol®, and Abraxane®. The solvent of Taxol® is a mixture of alcohol and cremophor, which is associated with a series of side effects such as allergic reactions, neutrophilic granulocytopenia, and bone marrow depression (Giuffrida et al., 2014). Abraxane® produces reduced systemic toxicity and side effects, but its tumor selectivity is weak and it lacks active targeting ability (Chen et al., 2015). Therefore, in this study we focused on optimizing the drug delivery system of PTX to strengthen its specificity.

A favorable nano-drug delivery system would be one that can target the tumor site with a decreased drug dosage but an enhanced drug concentration, and also reduce the toxicity resulting from PTX itself and the drug carrier. Solid lipid nanoparticles (SLNs) and nano-structured lipid carriers (NLCs) are two intensely explored lipid-based drug delivery systems. They have advantages including low toxicity, good biocompatibility and biodegradability

* Project supported by the Zhejiang Provincial Natural Science Foundation of China (No. LY14H160016)

# Electronic supplementary materials: The online version of this article (https://doi.org/10.1631/jzus.B1900624) contains supplementary materials, which are available to authorized users

ORCID: Xiao LIU, https://orcid.org/0000-0001-9048-4894

© Zhejiang University and Springer-Verlag GmbH Germany, part of Springer Nature 2020

(Yingchoncharoen et al., 2016). However, SLNs also have reported disadvantages including a highly ordered recrystallization of the particle structure after cooling, which usually results in low encapsulation, less controlled drug release, and physical instability (Noack et al., 2012). After addition of liquid lipids, the lipid distribution within the oil droplet is disturbed. Thus, an NLC could encapsulate more drug than an SLN and avoid drug leakage (Eskandani and Nazemiyeh, 2014; Esposito et al., 2017). However, SLNs and NLCs are easily internalized by the reticuloendothelial system (RES) and distributed to organs like the liver and spleen, which hinders drug accumulation in tumors.

Tumor targeting can be achieved by applying targeting molecules based on differences between tumor cells and normal cells at the molecular level, such as enhanced expression of folate receptor (Jones et al., 2017), transferrin receptor (Agrawal et al., 2017), and integrin αvβ3 (Quader et al., 2017) on tumor cells, and specific surface antigen programmed cell death protein 1 (PD-1) on lymphocytes (Hugo et al., 2016). Cluster determinant 44 (CD44) is a cell-membrane receptor which is over-expressed in many solid tumors compared with normal tissues (Cai et al., 2019). The CD44 protein is exclusively attached to the cell membrane and exists in many isoforms. Hyaluronic acid (HA) has a special interaction with CD44 that is highly expressed on the tumor cell surface. In contrast to tumor cells, the CD44 molecule on normal cells is usually in the un-activated mode in which its ability to bind with HA is far weaker (Chen et al., 2017; Kansu-Celik et al., 2017).

HA is a natural linear polysaccharide composed of a disaccharide unit formed by *N*-acetylgalactosamine or *N*-acetylglucosamine and uronic sugars. It is typically observed in the epithelial, connective, and nerve tissues of vertebrates (Knopf-Marques et al., 2016). It is a major component of normal extracellular matrix (ECM), but is also significantly elevated in several solid malignancies in which it is associated with increased interstitial pressures, reduced perfusion, and impaired delivery of therapeutic agents (Wong et al., 2017), and plays important roles in tumor progression. Extrinsic HA could bind to CD44 competitively with intrinsic HA molecules and then cut off the connection between the tumor cell and the ECM resulting in interrupted biological process. Thus, in this study HA was used to modify NLCs to target the anti-tumor drug PTX to the tumor site and finally eliminate the tumor.

## 2 Materials and methods

### 2.1 Materials

HA, with a molecular weight (MW) of 43.0 kDa, was purchased from the Shandong Freda Biotechnology Co., Ltd. (Shandong, China). Monostearin was purchased from the Shanghai Chemical Reagent Co., Ltd. (Shanghai, China). PTX was purchased from Shanghai Zhongxi Sunve (Shanghai, China). Octadecylamine (ODA) was purchased from Fluka™ of Honeywell Co., Ltd. (Charlotte, USA). Fluorescein isothiocyanate (FITC), oleic acid and 1-ethyl-3-(3-dimethylaminopropyl)carbodiimide (EDC) were supplied by Sigma Co., Ltd. (Louis, USA). Dulbecco's modified Eagle's medium (DMEM) was purchased from Gibco (BRL, USA). Fetal bovine serum was purchased from the Sijiqing Biology Engineering Materials Co., Ltd. (Zhejiang, China). Human breast cancer cell line MCF-7 was purchased from the Shanghai Institute of Cell Science, Chinese Academy of Sciences (Shanghai, China). 1-Hydroxy-5-pyrrolidinedione (NHS) was purchased from Shanghai Medpep Co., Ltd. (Shanghai, China). The alcohol and other reagents were all of analytical grade.

### 2.2 Synthesis of HA-ODA

HA (200 mg) was dissolved in a mixture of 15 mL of 2-(*N*-morpholino)ethanesulfonic acid (MES) buffer (10 mmol/L) and 10 mL of alcohol. After addition of EDC (480 mg), the mixture was activated for 1 h at 50 °C. After addition of NHS (58 mg), ODA dissolved in alcohol was dropped into the HA mixture and reacted for 12 h at 50 °C. A schematic of the synthesis process is presented in Fig. 1. The final reaction mixture was dialyzed in a dialysis bag (MW cutoff (MWCO)=7 kDa) against water for 48 h to remove soluble side products (Qiu et al., 2016). HA-ODA was produced after lyophilization.

### 2.3 Preparation of HA-ODA-modified NLCs (HA-NLCs)

NLCs were prepared using a modified aqueous solvent diffusion method as previously reported (Liu et al., 2016). Twenty-four milligrams of mono-stearin, 24 mg of soybean phospholipid, and 16 mg of oleic

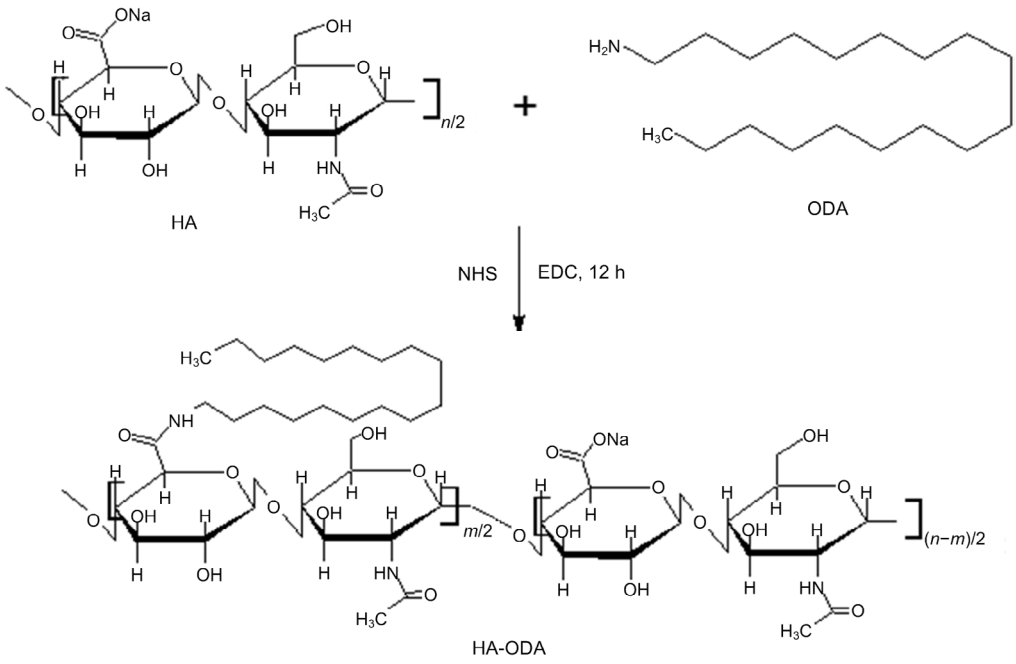


**Fig. 1 Synthesis scheme of hyaluronic acid-octadecylamine (HA-ODA)**
NHS: 1-hydroxy-5-pyrrolidinedione; EDC: 1-ethyl-3-(3-dimethylaminopropyl)carbodiimide

acid were mixed with 6.0 mL of alcohol and heated in a water bath at 60 °C. After dissolution, the alcohol mixture was injected into 30 mL of water under agitation at 400 r/min for 5 min. Then, the mixture was gradually cooled to room temperature, resulting in a suspension of NLC. The nanoparticles flocculated after the pH value was adjusted to its isoelectric point using diluted acetic acid (0.1 mol/L). The electrostatic repulsive force was disturbed with the addition of hydrogen ions. The nanoparticles were collected by centrifugation at 10000 r/min for 10 min. They were then re-suspended in water with polyvinyl alcohol (PVA; 0.01 g/mL) and the pH value was adjusted to 7.0. Drug-loaded NLCs (NLC/PTX) were prepared by dissolving PTX in the organic solvent at a feeding ratio of 5% (mass fraction). The HA-NLCs and HA-NLC/PTX were prepared by adding grafted HA-ODA (10%, mass fraction) into the organic phase mixed with a little formamide (100 μL formamide in 1 mL ethanol) to facilitate dissolution of the HA-ODA.

FITC was combined with ODA to produce a fluorescent probe. The reaction was carried out at room temperature and with stirring for 24 h in alcohol. Water was used to precipitate ODA-FITC and remove water-soluble FITC (Yuan et al., 2007). NLCs were labeled by adding the ODA-FITC probe (2%, mass fraction) to the organic phase during preparation.

## 2.4 Characterization of nanoparticles

The particle size, polydispersity index (PDI), and zeta potential of NLC, HA-NLC, NLC/PTX, and HA-NLC/PTX were determined by dynamic light scattering (3000HS, Malvern Instruments Co., Ltd., UK) after the concentration of the lipids was diluted to 100 μg/mL.

The PTX content was detected by high-performance liquid chromatography (HPLC; Agilent Technologies, USA). The mobile phase was water-acetonitrile (55:45, v/v). The mobile rate was set as 1.0 mL/min and the temperature as 35 °C. The ultraviolet detector was set to 227 nm. First, the nanoparticles NLC/PTX and HA-NLC/PTX were precipitated by adjusting to the isoelectric point by adding acetic acid (0.1 mol/L), and then the supernatant was collected after centrifugation at 20000 r/min for 30 min. HPLC, as described above, was used to measure the drug content of the supernatant. The drug encapsulation efficiency (EE) and drug loading (DL) values of PTX were calculated based on the difference between feeding and supernatant quantities as follows: EE%=[(weight of PTX in feed)−(weight of PTX in the supernatant)]/(weight of PTX in feed)×100%.

To study in vitro the release behavior of PTX-loaded NLC/PTX and HA-NLC/PTX, the precipitate

of PTX-loaded NLCs was re-dispersed in phosphate-buffered saline (PBS; pH 7.4) containing 2% Tween 80, which was used to provide a sink condition for the drug. Then the release system was put in an incubator shaker and shaken horizontally at 60 r/min and 37 °C. At predetermined time intervals (0, 1, 2, 4, 6, 8, 12, 24, and 48 h), 1 mL of the suspension was collected and ultra-filtered/centrifuged at 7000 r/min for 5 min. The identity of the filtrates was determined by the HPLC. The release profile of the PTX dispersion in PBS was obtained as a control ($n$=3).

### 2.5 Cellular internalization of the HA-NLCs

The cellular uptake of the nanoparticles was observed using confocal laser scanning microscopy (CLSM; IX81-FV1000, Olympus, Japan). Briefly, MCF-7 cells ($5\times10^4$ $mL^{-1}$) were seeded onto coverslips in a 24-well plate. After cultivation in an incubator for 24 h under 5% $CO_2$ at 37 °C, the cells were treated with ODA-FITC-labeled nanoparticles at a concentration of 20 μg/mL for 1, 2, 4, 8, or 12 h. The cell nuclei were stained by Hoechst 33342 solution for 15 min. The culture medium was discarded and the cells were washed three times with PBS. The cells were then fixed in 4% formaldehyde solution. CLSM was used for the semi-quantitative analysis of cellular internalization.

To study the competitive cell internalization inhibition, adherent cells were divided into two groups. One group was incubated with HA (50 μg/mL) for 0.5 h before adding NLC or HA-NLC nanoparticles. The other group was incubated with the culture medium. Subsequently, cells were further incubated for 1, 2, or 4 h followed by CLSM observation as above.

### 2.6 Cytotoxicity of PTX-loaded nanoparticles

3-(4,5-Dimethylthiazol-2-yl)-2,5-diphenyltetrazolium bromide (MTT) assay was adopted to determine the in vitro cytotoxicity of NLC/PTX and HA-NLC/PTX. MCF-7 cells were seeded in 96-well culture plates at a density of $5\times10^3$ cells/well and cultured for 24 h in the incubator. Formulations containing PTX were added to the 96-well culture plates, including various concentrations of free PTX, NLC/PTX, and HA-NLC/PTX. Blank culture medium served as a blank control. After 48 h, 20 μL of MTT solution (5.0 mg/mL) was added to each well and the cells were further cultivated for 4 h. Then, the culture medium was discarded, and 200 μL of dimethyl sulphoxide (DMSO) was used to dissolve the purple formazan crystals. A micro-plate reader (Bio-Rad, Model 680, USA) was used to measure the absorbance of each well at 570 nm. Cell viability was calculated in reference to the cells incubated with blank culture medium. The cell survival rate curves were plotted from the data of triplicate assays.

### 2.7 In vivo distribution of the NLCs

The strain of mice used was BALB/c nude. 1,1-Dioctadecyl-3,3,3',3'-tetramethylindotricarbocyanine-iodide (DiR), a near infrared dye, was encapsulated in NLCs and HA-NLCs forming NLC/DiR and HA-NLC/DiR, which were prepared as PTX-loaded nanoparticles to trace NLCs and HA-NLCs in vivo, respectively. The xenografted tumor mice model was established on the female nude mice (6–8 weeks). A suspension of about $5.0\times10^6$ MCF-7 cells was inoculated subcutaneously in the mice. When the tumor size reached 500 $mm^3$, 0.2 mL of NLC/DiR or HA-NLC/DiR suspension was injected into the tail vein to investigate the bio-distribution and tumor targeting ability. At pre-defined time points (2, 12, 24, 48, and 72 h) after injection, fluorescence signals of the mice were observed using an in vivo fluorescence imaging system called Maestro (CRI Inc., USA). The excitation wavelength was set at 704 nm and the range of emission wavelength was set from 740 to 950 nm.

### 2.8 Statistical analysis

The results are displayed as mean±standard deviation and were analyzed by $t$-tests. Differences were considered statistically significant when the $P$-value was <0.05.

## 3 Results and discussion

### 3.1 Physicochemical properties of the NLCs

In general, HA-ODA was synthesized as illustrated in Fig. 1. An amide bond was formed between the carboxyl groups of water-soluble HA and the amino groups of ODA. The HA-ODA was assumed to contain one HA molecule and one ODA molecule, as the feeding ratio was 1:1 when performing the reaction. Thus, one side of the HA was hydrophobic and the other side hydrophilic. The $^1$H nuclear magnetic

resonance (NMR) spectra (Fig. 2) of the chemicals were used to verify the chemical structure of HA-ODA. In the $^1$H NMR spectrum of HA-ODA, peaks at about 1.2 ppm (parts per million) were attributed to protons of the $–CH_2–$ group of ODA, and peaks at 2.5 ppm were attributed to protons of the newly formed amide –NHCO–. These results confirmed that HA-ODA was successfully synthesized.

When preparing NLCs, HA-ODA was dissolved in the organic solution and fully mixed with the solid and liquid lipids. When the organic solution was injected into the water phase, the hydrophobic side would insert to the lipid core while the hydrophilic side, the HA chain, would spread over the surface of the nanoparticle. Thus, the HA-NLC nanoparticle was achieved.

The particle size and zeta potential are shown in Table 1. The size increased after PTX was encapsulated. HA modification increased the particle size and decreased the zeta potential, which were attributed to the HA distribution and its carboxyl groups, respectively. The medium PDI value and zeta potential (Fig. S1) demonstrated uniform and narrowly distributed particles.

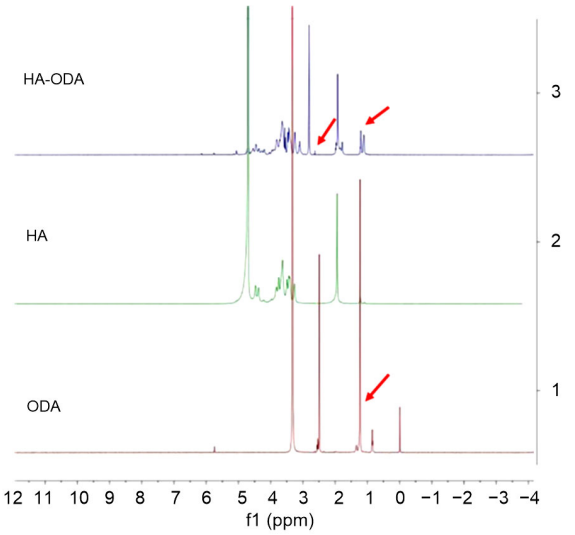


**Fig. 2 $^1$H NMR spectra of HA-ODA, HA, and ODA**
The arrows indicate the peaks at 1.2 and 2.5 ppm. NMR: nuclear magnetic resonance; HA: hyaluronic acid; ODA: octadecylamine; ppm: parts per million

Quantitatively determined by HPLC, the DL was (3.79±0.22)% for NLC/PTX and (3.71±0.43)% for HA-NLC/PTX. The EE was (73.30±1.76)% for NLC/PTX and (72.00±2.34)% for HA-NLC/PTX. It appears that the encapsulation of the PTX molecules in the NLC was attributed to the mixed soybean lipids and liquid oleic acid, which enlarged the space for drugs in the droplet. The HA modification had no influence on the DL or EE of PTX.

It was important to evaluate the physical stability of the HA-NLC/PTX, HA-NLC, and NLC. When preparing these nanoparticles, we measured their zeta potential, size, PDI, and drug content every ten days. Table 1 shows the results from measurements made on the day they were prepared, and Table 2 shows the results from measurements made ten days later. After ten days at room temperature, the particle size of NLC and NLC/PTX increased (Table 2, Fig. S2). The drug content decreased because of drug release into the surrounding water medium. The particle size of HA-NLC and HA-NLC/PTX also increased, but to a lesser extent. As time went on, flocculation occurred in the colloidal system of NLC/PTX. The hydrophilic HA chain surrounding the HA-NLC particle stabilized the particle to some extent. Thus, it may be better to preserve the NLC/PTX and HA-NLC/PTX in the form of freeze-dried powder, but the ability of the NLC/PTX and HA-NLC/PTX powder to re-dissolve should be investigated.

**Table 1 Particle size and zeta potential of the NLCs on the day they were prepared**

| Sample | $d$ (nm) | $\zeta$ (mV) | PDI |
|---|---|---|---|
| NLC | 36.9±6.1 | −17.8±1.3 | 0.306±0.043 |
| NLC/PTX | 52.1±4.4 | −19.5±0.8 | 0.319±0.055 |
| HA-NLC | 48.9±4.8 | −22.3±2.1 | 0.309±0.019 |
| HA-NLC/PTX | 75.8±11.5 | −25.4±3.2 | 0.289±0.039 |

$d$: diameter; $\zeta$: zeta potential; NLC: nano-structured lipid carrier; PTX: paclitaxel; HA-NLC: hyaluronic acid-octadecylamine (HA-ODA)-modified NLC; PDI: polydispersity index. Data were expressed as mean±standard deviation (SD) ($n$=3)

**Table 2 Particle size and zeta potential of the NLCs ten days after they were prepared**

| Sample | $d$ (nm) | PDI | $\zeta$ (mV) | Drug content (%) |
|---|---|---|---|---|
| NLC | 100.1±10.1 | 0.410±0.201 | −10.8±4.3 | |
| NLC/PTX | 150.5±12.4 | 0.654±0.154 | −5.5±3.2 | 1.04±0.67 |
| HA-NLC | 68.8±5.0 | 0.353±0.083 | −18.8±2.5 | |
| HA-NLC/PTX | 90.5±12.4 | 0.415±0.054 | −16.8±4.3 | 1.45±0.58 |

$d$: diameter; $\zeta$: zeta potential; NLC: nano-structured lipid carrier; PTX: paclitaxel; HA-NLC: hyaluronic acid-octadecylamine (HA-ODA)-modified NLC; PDI: polydispersity index. Data were expressed as mean±SD ($n$=3)

The drug release behavior is shown in Fig. 3. Drug release from the encapsulated PTX was hindered compared to that from free PTX solution. The peripheral HA layer also had a small impact in delaying drug release. At 24 h, the accumulated percentage drug release was 64.0% from NLC/PTX and 49.1% from HA-NLC/PTX.

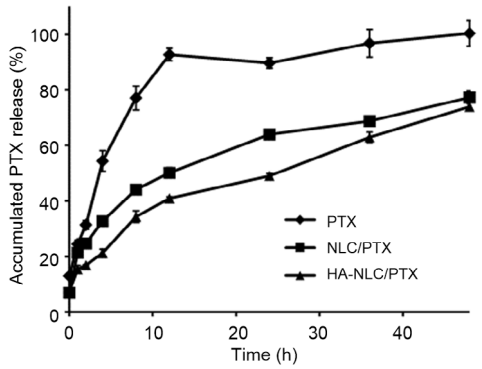


**Fig. 3 In vitro release profiles of PTX suspension, NLC/PTX and HA-NLC/PTX**
PTX: paclitaxel; NLC: nano-structured lipid carrier; HA-NLC: hyaluronic acid-octadecylamine (HA-ODA)-modified NLC. Data were expressed as mean±SD ($n$=3)

### 3.2 Cellular internalization of NLCs

The in vitro cellular uptake of NLCs by MCF-7 cells, which had highly expressed CD44 molecules (Qiu et al., 2017), was used to verify the targeting ability of HA-NLC. The ODA-FITC fluorescence probe could insert into the lipid core of the NLCs through its hydrophobic chain and make the NLCs traceable. After incubation for 1 h, cells co-cultured with NLC or HA-NLC showed obvious fluorescence, and the fluorescence intensity became stronger as the incubation time extended (Fig. 4). There was almost no difference between the fluorescence intensity of NLCs and that of HA-NLCs, owing mainly to the super strong cellular internalization ability of all types of NLCs. There was almost no fluorescence in the cell nucleus, indicating that almost all HA-NLCs were

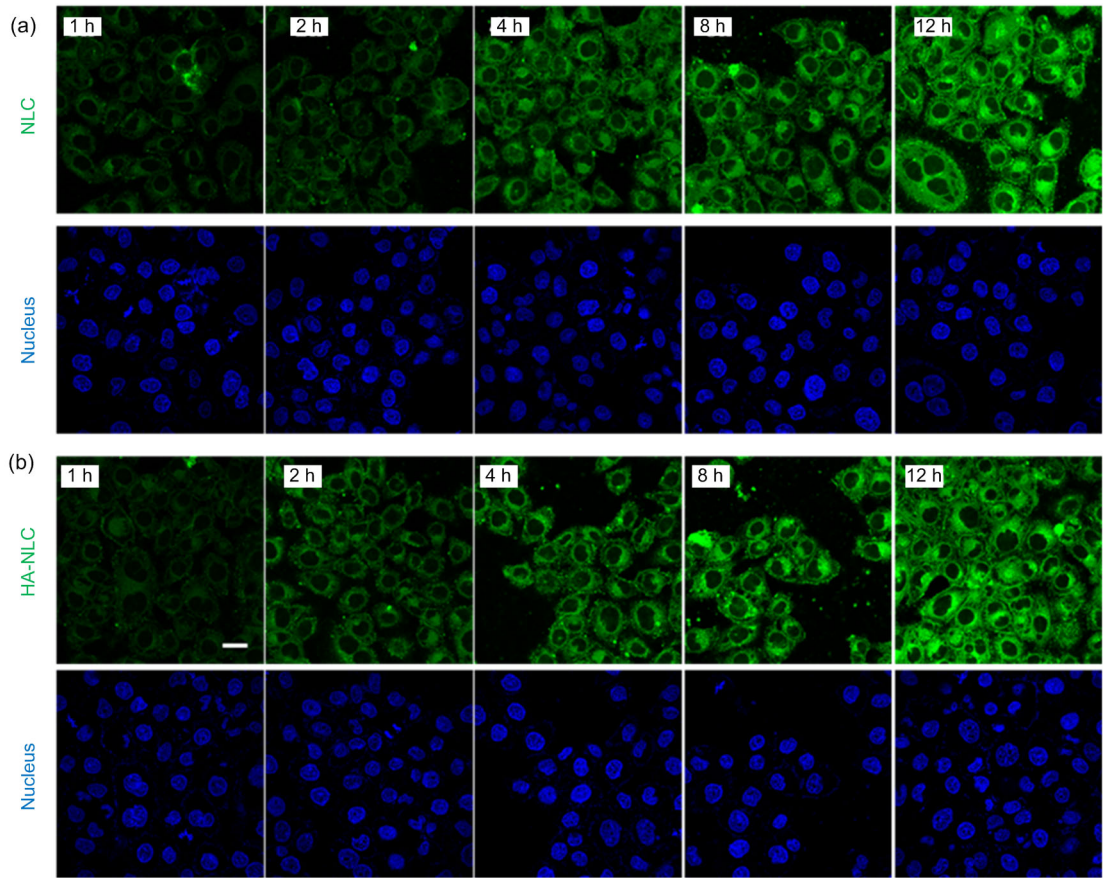


**Fig. 4 CLSM images of the cellular uptake of ODA-FITC labeled NLCs (a) and HA-NLCs (b) on MCF-7 cells**
CLSM: confocal laser scanning microscopy; ODA: octadecylamine; FITC: fluorescein isothiocyanate; NLC: nano-structured lipid carrier; HA-NLC: hyaluronic acid-ODA-modified NLC. Scale bar=20 μm

distributed in the cytoplasm, which is the exact target site for the drug PTX. The HA-NLCs were able to concentrate PTX in its acting site, thereby improving the drug efficiency.

To further explore the effect of HA on cellular internalization, a competitive internalization assay was performed. Pre-incubation with HA resulted in a reduction in the fluorescence intensity of HA-NLCs (Fig. 5), indicating that part of the HA-NLC internalization was mediated by the CD44 receptors. The HA-NLCs could recognize CD44 and were then endocytosed into the tumor cells. This could assist in overcoming drug resistance by avoiding efflux pumps.

### 3.3 Cytotoxicity of HA-NLC/PTX

In consideration of the poor solubility of PTX and its tendency to dissolve out when added to the cell culture medium, Taxol®, which has a strong tumor inhibition effect, was adopted as the positive control.

The $IC_{50}$ (half maximal inhibitory concentration) values calculated from the survival rate curves of cells were (0.79±0.07), (0.33±0.02), and (0.29±0.02) μg/mL for Taxol®, NLC/PTX, and HA-NLC/PTX, respectively (Fig. 6). The PTX encapsulated in NLCs and HA-NLCs showed a stronger inhibition effect than Taxol®, which may have been attributable to the excellent cellular uptake. The fast cellular uptake may also be the reason why no significant differences in cytotoxicity were observed between NLCs and HA-NLCs.

A drug carrier is needed which does no harm to normal cells or their function. The cytotoxicity of HA-NLC on MCF-7 cells was determined by MTT assay. The survival rate of the cells hardly changed when the concentration of HA-NLC was increased from 50 to 500 μg/mL (Fig. 7). Even when the concentration was increased to 500 μg/mL, the cell survival rate was still 85.5%, indicating the high safety of the carrier.

### 3.4 In vivo distribution of HA-NLC

DiR is a kind of hydrophobic near-infrared dye that can be encapsulated in NLCs to trace their distribution in the animal body. The NLCs accumulated in the liver and spleen very fast and remained there for a very long time (Fig. 8). Even 72 h after administration, the fluorescence was still strong. The aggregation of HA-NLCs in the liver and spleen was also obvious after 2 h. However, the fluorescence signal also emerged in the tumor site, and the fluorescence intensity of the tumor became stronger with time, indicating that more and more HA-NLCs were gathering at the tumor site. At 72 h after administration, still no or very weak fluorescence of NLCs was noticeable at the tumor site, but fluorescence intensity was evident for HA-NLCs. The in vivo images show that HA could serve as a targeting molecule to delivery NLCs to tumors.

HA has application in targeting preparations because of its good biocompatibility, biodegradability,

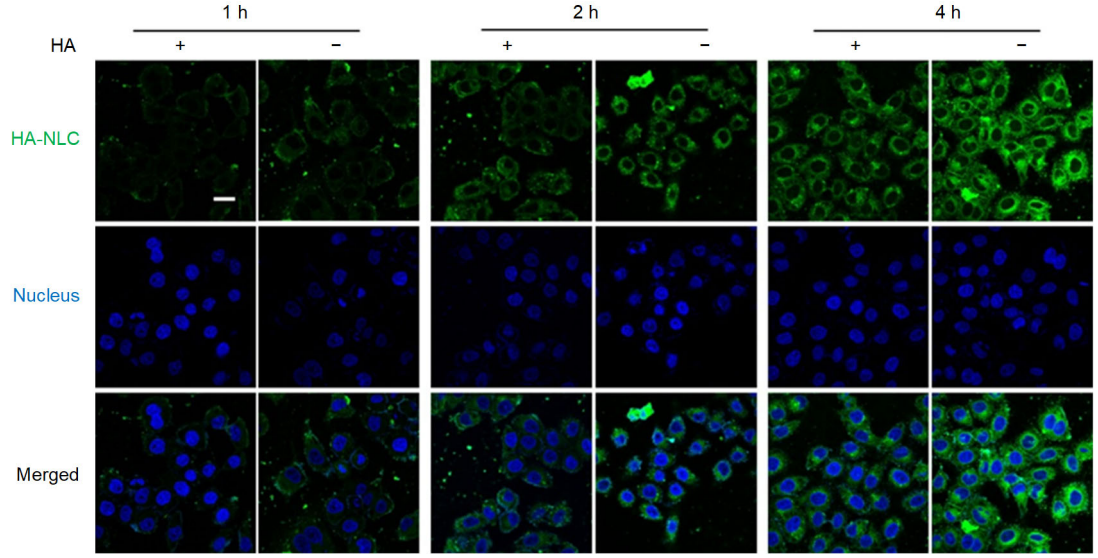


**Fig. 5 CLSM images of HA-NLC cellular uptake with (+) or without (−) pre-incubation of HA**

CLSM: confocal laser scanning microscopy; HA-NLC: hyaluronic acid-octadecylamine (HA-ODA)-modified nano-structured lipid carrier. Scale bar=20 μm

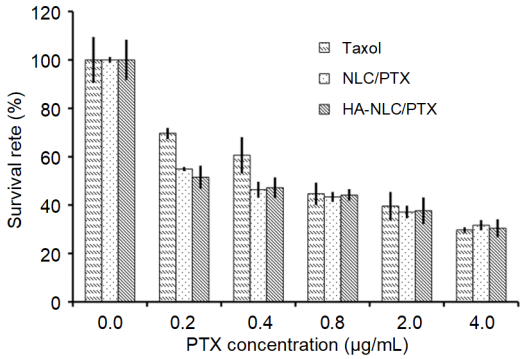


**Fig. 6 Survival rates of MCF-7 cells following treatment with Taxol®, NLC/PTX, or HA-NLC/PTX**
NLC: nano-structured lipid carrier; PTX: paclitaxel; HA-NLC: hyaluronic acid-octadecylamine (HA-ODA)-modified NLC. Data were expressed as mean±SD ($n$=3)

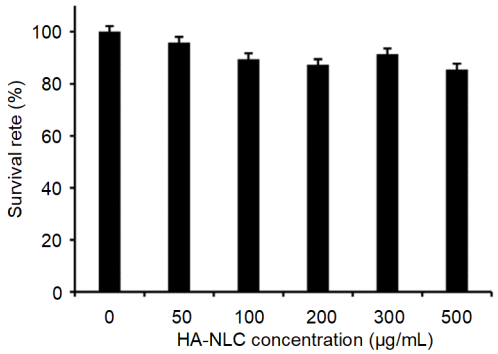


**Fig. 7 Survival rate of MCF-7 cells with different concentrations of HA-NLC**
HA-NLC: hyaluronic acid-octadecylamine (HA-ODA)-modified nano-structured lipid carrier. Data were expressed as mean±SD ($n$=3)

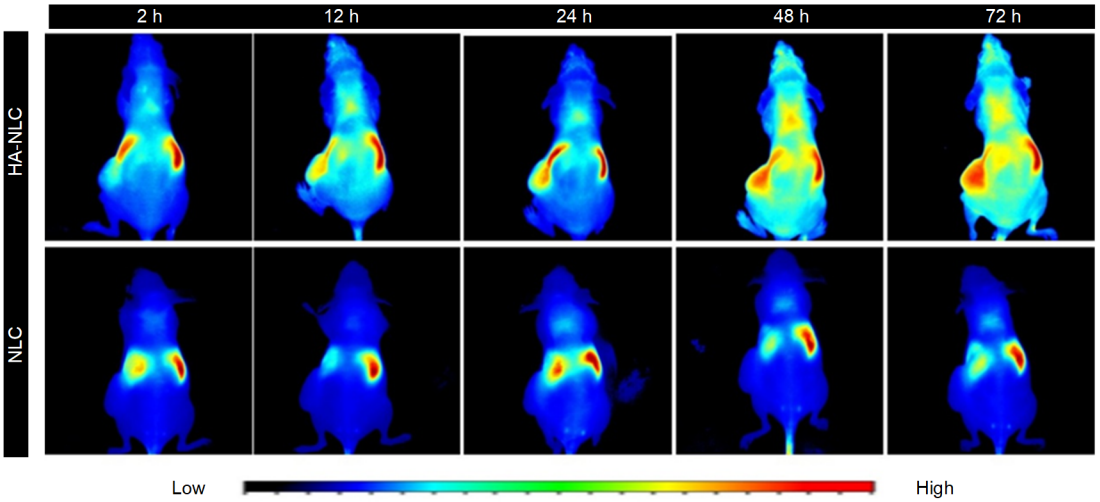


**Fig. 8 In vivo bio-distribution images of DiR-loaded NLC and HA-NLC nanoparticles in tumour-bearing nude mice**
Tumors were on the left side. DiR: 1,1-dioctadecyl-3,3,3'3'-tetramethylindotricarbocyanine-iodide; NLC: nano-structured lipid carrier; HA-NLC: hyaluronic acid-octadecylamine (HA-ODA)-NLC

endogenous substance, and specific recognition and binding capacity for CD44 molecules (Qiu et al., 2013; Wickens et al., 2017; Chen et al., 2018). For example, it has been used to construct a micelle by synthesis of an amphiphilic graft (Zhong et al., 2016; Zhang et al., 2017), or absorbed onto the surface of a kind of positively charged NLC utilizing its electronegativity (Tran et al., 2014; Martens et al., 2017). In this research, we first explored the ability of HA-ODA to insert into NLCs through its hydrophobic chain of eighteen carbons, thereby protecting HA from separation from the NLCs and enhancing its targeting ability. Unlike HA absorption by electrostatic interaction, this HA-ODA insert would not result in an obvious increase of particle size or uneven particle size distribution. We speculate that the HA was symmetrically distributed on the surface of NLCs and that this may have been attributable to the one step preparation by adding HA-ODA to the organic solution and fully mixing with other lipids.

## 4 Conclusions

In this research, HA-ODA was synthesized and used to modify NLCs by inserting in the lipid core through the hydrophobic ODA chain. The insoluble drug PTX could be encapsulated and showed stronger

antitumor efficiency than Taxol®. The HA-NLCs had strong internalization in CD44 highly expressed MCF-7 cells and decreased the distribution of NLCs in the liver and spleen. Furthermore, HA enhanced its distribution to CD44 highly expressed tumors. The results suggest that HA could be adopted as a targeting molecular to modify NLCs and that HA-NLCs represent a stable and strong targeting drug delivery system with potential for future applications.

## Contributors

Xiao LIU performed the experimental research, analyzed the data, and wrote the manuscript. Hai LIU contributed to the study design and data analysis. Su-lan WANG performed the establishment of animal models. Jing-wen LIU wrote and edited the manuscript. All authors have read and approved the final manuscript and, therefore, have full access to all the data in the study and take responsibility for the integrity and security of the data.

## Compliance with ethics guidelines

Xiao LIU, Hai LIU, Su-lan WANG, and Jing-wen LIU declare that they have no conflict of interest.

All the animal studies were conducted according to the guidelines issued by the Ethical Committee of Zhejiang University, Hangzhou, China (Ethical Approval No. 14481) and all animal experiments complied with the National Institutes of Health Guide for the Care and Use of Laboratory Animals (NIH Publications No. 8023, revised 1978).

## References

Agrawal M, Ajazuddin, Tripathi DK, et al., 2017. Recent advancements in liposomes targeting strategies to cross blood-brain barrier (BBB) for the treatment of Alzheimer's disease. *J Control Release*, 260:61-77. https://doi.org/10.1016/j.jconrel.2017.05.019

Bourgeois-Daigneault MC, St-Germain LE, Roy DG, et al., 2016. Combination of paclitaxel and MG1 oncolytic virus as a successful strategy for breast cancer treatment. *Breast Cancer Res*, 18(1):83. https://doi.org/10.1186/s13058-016-0744-y

Cai J, Fu JF, Li RR, et al., 2019. A potential carrier for anti-tumor targeted delivery-hyaluronic acid nanoparticles. *Carbohydr Polym*, 208:356-364. https://doi.org/10.1016/j.carbpol.2018.12.074

Chen HR, Huang XW, Wang ST, et al., 2015. Nab-paclitaxel (abraxane)-based chemotherapy to treat elderly patients with advanced non-small-cell lung cancer: a single center, randomized and open-label clinical trial. *Chin J Cancer Res*, 27(2):190-196. https://doi.org/10.3978/j.issn.1000-9604.2014.12.17

Chen J, Ouyang J, Chen QJ, et al., 2017. EGFR and CD44 dual-targeted multifunctional hyaluronic acid nanogels boost protein delivery to ovarian and breast cancers in vitro and in vivo. *ACS Appl Mater Interfaces*, 9(28): 24140-24147. https://doi.org/10.1021/acsami.7b06879

Chen Z, Deng S, Yuan D, et al., 2018. Novel nano-microspheres containing chitosan, hyaluronic acid, and chondroitin sulfate deliver growth and differentiation factor-5 plasmid for osteoarthritis gene therapy. *J Zhejiang Univ-Sci B (Biomed & Biotechnol)*, 19(12):910-923. https://doi.org/10.1631/jzus.B1800095

Eskandani M, Nazemiyeh H, 2014. Self-reporter shikonin-Act-loaded solid lipid nanoparticle: formulation, physicochemical characterization and geno/cytotoxicity evaluation. *Eur J Pharm Sci*, 59:49-57. https://doi.org/10.1016/j.ejps.2014.04.009

Esposito E, Drechsler M, Mariani P, et al., 2017. Lipid nanoparticles for administration of poorly water soluble neuroactive drugs. *Biomed Microdevices*, 19(3):44. https://doi.org/10.1007/s10544-017-0188-x

Giuffrida MC, Dosio F, Castelli F, et al., 2014. Lipophilic prodrug of paclitaxel: interaction with a dimyristoylphosphatidylcholine monolayer. *Int J Pharm*, 475(1-2):624-631. https://doi.org/10.1016/j.ijpharm.2014.09.022

Hugo W, Zaretsky JM, Sun L, et al., 2016. Genomic and transcriptomic features of response to anti-PD-1 therapy in metastatic melanoma. *Cell*, 165(1):35-44. https://doi.org/10.1016/j.cell.2016.02.065

Jones SK, Sarkar A, Feldmann DP, et al., 2017. Revisiting the value of competition assays in folate receptor-mediated drug delivery. *Biomaterials*, 138:35-45. https://doi.org/10.1016/j.biomaterials.2017.05.034

Kansu-Celik H, Gungor M, Ortac F, et al., 2017. Expression of CD44 variant 6 and its prognostic value in benign and malignant endometrial tissue. *Arch Gynecol Obstet*, 296(2): 313-318. https://doi.org/10.1007/s00404-017-4430-9

Knopf-Marques H, Pravda M, Wolfova L, et al., 2016. Hyaluronic acid and its derivatives in coating and delivery systems: applications in tissue engineering, regenerative medicine and immunomodulation. *Adv Healthc Mater*, 5(22):2841-2855. https://doi.org/10.1002/adhm.201600316

Liu JW, Meng TT, Yuan M, et al., 2016. MicroRNA-200c delivered by solid lipid nanoparticles enhances the effect of paclitaxel on breast cancer stem cell. *Int J Nanomed*, 11:6713-6725. https://doi.org/10.2147/IJN.S111647

Martens TF, Peynshaert K, Nascimento TL, et al., 2017. Effect of hyaluronic acid-binding to lipoplexes on intravitreal drug delivery for retinal gene therapy. *Eur J Pharm Sci*, 103:27-35. https://doi.org/10.1016/j.ejps.2017.02.027

Noack A, Hause G, Mäder K, 2012. Physicochemical characterization of curcuminoid-loaded solid lipid nanoparticles. *Int J Pharmaceut*, 423(2):440-451. https://doi.org/10.1016/j.ijpharm.2011.12.011

Qiu LP, Long MM, Chen DW, 2013. Hyaluronic acid-based

carriers for tumor targeted delivery system. *Acta Pharm Sin*, 48(9):1376-1382 (in Chinese). https://doi.org/10.16438/j.0513-4870.2013.09.001

Qiu LP, Zhu MQ, Huang Y, et al., 2016. Mechanisms of cellular uptake with hyaluronic acid-octadecylamine micelles as drug delivery nanocarriers. *RSC Adv*, 6(46):39896-39902. https://doi.org/10.1039/C5RA27532F

Qiu LP, Zhu MQ, Gong K, et al., 2017. pH-triggered degradable polymeric micelles for targeted anti-tumor drug delivery. *Mater Sci Eng C*, 78:912-922. https://doi.org/10.1016/j.msec.2017.04.137

Quader S, Liu X, Chen Y, et al., 2017. cRGD peptide-installed epirubicin-loaded polymeric micelles for effective targeted therapy against brain tumors. *J Control Release*, 258:56-66. https://doi.org/10.1016/j.jconrel.2017.04.033

Tran TH, Choi JY, Ramasamy T, et al., 2014. Hyaluronic acid-coated solid lipid nanoparticles for targeted delivery of vorinostat to CD44 overexpressing cancer cells. *Carbohydr Polym*, 114:407-415. https://doi.org/10.1016/j.carbpol.2014.08.026

Wickens JM, Alsaab HO, Kesharwani P, et al., 2017. Recent advances in hyaluronic acid-decorated nanocarriers for targeted cancer therapy. *Drug Dis Today*, 22(4):665-680. https://doi.org/10.1016/j.drudis.2016.12.009

Wong KM, Horton KJ, Coveler AL, et al., 2017. Targeting the tumor stroma: the biology and clinical development of pegylated recombinant human hyaluronidase (PEGPH20). *Curr Oncol Rep*, 19(7):47. https://doi.org/10.1007/s11912-017-0608-3

Yingchoncharoen P, Kalinowski DS, Richardson DR, 2016. Lipid-based drug delivery systems in cancer therapy: what is available and what is yet to come. *Pharmacol Rev*, 68(3):701-787. https://doi.org/10.1124/pr.115.012070

Yuan H, Chen J, Du YZ, et al., 2007. Studies on oral absorption of stearic acid SLN by a novel fluorometric method. *Colloids Surf B Biointerfaces*, 58(2):157-164. https://doi.org/10.1016/j.colsurfb.2007.03.002

Zhang HB, Li W, Guo XM, et al., 2017. Specifically increased paclitaxel release in tumor and synergetic therapy by a hyaluronic acid-tocopherol nanomicelle. *ACS Appl Mater Interfaces*, 9(24):20385-20398. https://doi.org/10.1021/acsami.7b02606

Zhong YN, Goltsche K, Cheng L, et al., 2016. Hyaluronic acid-shelled acid-activatable paclitaxel prodrug micelles effectively target and treat CD44-overexpressing human breast tumor xenografts in vivo. *Biomaterials*, 84:250-261. https://doi.org/10.1016/j.biomaterials.2016.01.049

## List of electronic supplementary materials

Fig. S1 Zeta potential determination of the nanoparticles (NLC, NLC/PTX, HA-NLC, and HA-NLC/PTX)

Fig. S2 Size distribution of the nanoparticles (NLC, NLC/PTX, HA-NLC, and HA-NLC/PTX) at the 10th day after they were prepared

## 中文概要

**题　目：透明质酸衍生物修饰脂质纳米载体的抗肿瘤作用及体内靶向研究**

**目　的：**以脂质纳米载体为递药系统向肿瘤部位靶向输送难溶性抗肿瘤药物紫杉醇，实现药物的靶向递送。

**创新点：**采用一端疏水化的透明质酸修饰脂质纳米载体，利用透明质酸与肿瘤部位高表达 CD44 的特异性结合，实现载药脂质纳米粒的靶向输送。

**方　法：**通过酰胺反应，将硬脂胺化学嫁接至透明质酸，制备透明质酸-硬脂胺嫁接物。采用水性溶剂扩散法制备脂质纳米粒，并将透明质酸-硬脂胺嫁接物插入脂质纳米粒的表面。使用红外染料 DiR 标记脂质纳米粒，通过小动物活体成像技术观察标记脂质纳米粒的体内分布。

**结　论：**透明质酸修饰的脂质纳米粒，可通过与 CD44 的特异性结合，实现抗肿瘤药物的靶向递送。

**关键词：**紫杉醇；透明质酸-硬脂胺；纳米结构脂质载体；肿瘤靶向；体内分布